Spatial variability of deep-ocean motions above an abyssal plain

Hans van Haren

Royal Netherlands Institute for Sea Research (NIOZ), Den Burg, Netherlands

Received 25 June 2004; revised 23 September 2004; accepted 19 October 2004; published 14 December 2004.

[1] Near-bottom current observations are discussed from an array of moorings separated by 8–40 km horizontally in the Madeira abyssal plain, North Atlantic Ocean. The area is topographically smooth, but observed currents varied strongly over short distances. Across horizontal scales O(10 km), "incoherent" internal wave properties were retrieved such as conservation of relative frequency bandwidth and internal wave polarization at inertial, tidal, and higher harmonics frequencies. In the vertical (between 10–110, 110–650 m above the bottom (mab) at ~5000 m), the current differences (~shear) were predominantly at the local inertial frequency f. Near f the largest variance was found at 110 mab, with peaks in power at 0.99f and 1.03f. As stratification was weak ($N \approx 2f$) the subinertial frequency peak was well within the combined internal inertio-gravity wave band. At 650 mab, $N \approx 4f$, and smaller peaks at ~1.00f and 1.03f were observed. Toward the bottom subinertial currents increased in magnitude. The horizontal scale of variation of subinertial and inertial motions was small: ~30 km. The magnitude of horizontal current differences in these frequency bands was equal to that in the tidal band. Although the energetically dominant, highly deterministic tidal currents were predominantly barotropic, confirming a previous study, their horizontal scale of variation was ~300 km, due to small bottom relief. Results are discussed relevant for matching records from nearby moorings, to generate extra long time series. *INDEX TERMS:* 4544 Oceanography: Physical: Internal and inertial waves; 4560 Oceanography: Physical: Surface waves and tides (1255); 4508 Oceanography: Physical: Coriolis effects; *KEYWORDS:* internal waves, near-inertial motions, wave trapping

Citation: van Haren, H. (2004), Spatial variability of deep-ocean motions above an abyssal plain, *J. Geophys. Res.*, *109*, C12014, doi:10.1029/2004JC002558.

1. Introduction

[2] After many studies on internal waves in the 1970s and 1980s and following the suggestion that internal wave-induced mixing can dominate the large-scale meridional overturning circulation in the ocean [*Munk and Wunsch*, 1998], studies on waves in the ocean interior have recently received a revived interest. Of particular interest here are the dominant spatial scales associated with internal waves, since these scales are important for mixing. Knowledge of vertical scales is important for vertical current variability, or shear, and advection. Shear instability is one of the dominant processes for diapycnal mixing. Horizontal scales also affect nonlinear advection, which in extreme cases causes a wave to overturn and thus mix when $u/c \rightarrow 1$, u denoting the particle velocity and c denoting the phase speed of a wave. So far, very few comprehensive observational studies were performed on deep-ocean spatial scale variability over a prolonged period of time O(months), so that all relevant (internal wave) frequencies were well resolved in a statistical sense. An exception was a 7-month study by IOS-Wormley using six moorings at 8–40 km distance in the Madeira abyssal plain in 1980–1981 [*Saunders*, 1983] (hereinafter S83). Here these historic data are re-examined from a different viewpoint focusing on the effects of spatial variability in currents in different frequency (σ) bands, as evidenced from spectral analysis. The focus is on tidal and inertial bands and on nonlinear incoherent internal waves. The reason for this study is also practical: We are interested in (problems in) generating long time series by matching records from moorings located nearby and consecutively in time. The question is whether such series can thus be used to establish the spatial variability of dominant internal wave motions, not just from a statistical viewpoint.

[3] Previously, a few short-period O(weeks) observational studies attempted to establish the vertical coherence scale of internal waves [*Siedler*, 1971; *Webster*, 1972] and the horizontal coherence scale [*Siedler*, 1974]. These statistical studies, using 10–40 days of data from North Atlantic site D between ~100 and 2000 m depth, were confirmed with the single comprehensive internal wave scale study to date: the IWEX experiment [*Briscoe*, 1975]. During IWEX, horizontal and vertical scales between 1.4 and 1600 m were studied for 40 days between 600 and 2200 m depth in a nearly motionless triangular mooring array in 5400 m water depth in the MODE area where tidal currents are weak. The focus in all these studies was on the establishment of the cutoff internal wave frequency $\sigma_{0.5}$, at which coherence dropped below 0.5 as a function of separation distance between sensors. Observational results were compared with suggestions on internal wave statistics by *Garrett and Munk* [1972]

0148-0227/04/2004JC002558$09.00

(hereinafter GM). The data records were rather short for a proper resolution of low-frequency near-inertial internal waves. Specific frequency bands such as near-inertial and tidal bands were not considered in the coherency analysis. Nevertheless, the main results of these observations were, for vertical coherence dropping to a value of 0.5 across a vertical interval Δz (in m) at frequency [*Webster*, 1972],

$$\sigma_{z,0.5} = 312/\Delta z[\mathrm{cpd}], \quad (1)$$

expressing frequency in cycles per day (1 cpd = $2\pi/86400\,\mathrm{s}^{-1}$). The limiting frequency (1) was found to coincide with the minimum buoyancy frequency N_{min} of the total water column $-H < z < 0$, where H is the water depth, $N_{min} = \min[N(z)] = \min[(g/\rho\Delta\rho/\Delta z)^{0.5}]$, N is the local buoyancy frequency, g is the acceleration of gravity, and ρ is density, for finite differences Δ and vertical separation distances $\Delta z > 10$ m [*Siedler*, 1971; *Webster*, 1972]. When $\Delta z < 10$ m, $N_{min} \rightarrow N$. This result was attributed to a change in the spread of order of internal wave modes for motions at frequencies spanning the entire water column ($\sigma < N_{min}$) and those being local ($N_{min} < \sigma < N$) [*Siedler*, 1971]. For horizontal coherence dropping to a value of 0.5 across a horizontal interval Δx (in m) at frequency [*Briscoe*, 1975],

$$\sigma_{x,0.5} = 7920/\Delta x[\mathrm{cpd}], \quad (2)$$

which compared well with N(z) at each of the depth levels investigated, suggesting horizontal isotropy of the internal wave field. Although *Briscoe* [1975] listed some cautionary notes on the use of (coherence) statistics to describe internal waves, he clearly demonstrated with his unique data set that the disparity between temperature and current coherences from the same set of sensors was not due to instrumental errors. From very closely ($\sim$6 m horizontally) spaced instruments it was concluded that current meters showed very high signal/noise ratios at internal wave frequencies. As ''noise levels'' increased for larger separation distances, this noise was not instrumental, and *Briscoe* [1975] suggested invoking internal wave nonlinearity to describe such noise. As will be demonstrated in the present paper, nonlinearity also dominates internal wave motions near the bottom of a deep-ocean abyssal plain, as was recently found down the continental slope of the Bay of Biscay [*van Haren et al.*, 2002].

[4] The 225 days of measurements from the Madeira abyssal plain were from current meters relatively far apart considering (1) and (2) (Figure 1 and Table 1; (100 and) 540 m in the vertical, so that following (1), $\sigma_{z,0.5} = 0.6$ cpd $< f$ outside the bottom boundary layer, and >8 km in the horizontal, so that following (2), $\sigma_{x,0.5} < 1.0$ cpd $\approx f$. The local inertial frequency $f = 2\Omega\sin\varphi$, the vertical component of the Earth's rotational vector of magnitude Ω measured at latitude φ. As a result, vertical and horizontal coherency between different records was not expected statistically significant, as in general the distances were larger for all internal wave band frequencies ($\sigma_{z,0.5} = f$ for $z \approx 300$ m following (1); $\sigma_{x,0.5} = f$ for $x \approx 8$ km following (2)). However, as we shall see, such general statistics do not entirely apply for motions at particular frequencies. This is easily understood for barotropic tides, which are coherent over large scales. More difficult to understand is the possible variability in coherency near an internal tidal wave source, for example near a shelf break.

[5] S83 mainly considered data from 10 m above the bottom (mab) for three bands of motions: the semidiurnal tidal band, the inertial band, and the subinertial (low-frequency) band. He found that the semidiurnal band was dominated (>90% in variance) by barotropic or coherent baroclinic motions, and that subinertial motions were bottom intensified. The latter varied across relatively short horizontal distances of $\sim$35 km, evidence of turbulent rather than wave-like motions varying on 30- to 60- and $\sim$100-day timescales. For near-inertial motions, S83 found a 3-km wavelength in the vertical and 100 km in the horizontal, which is much larger than expected for the internal wave band from (1) and (2). These waves primarily propagated upward, as was concluded from the observation of largest energy at 100 mab. It was also suggested that they propagated to the south, apparently generated by $\sim$300-m-high ridges some 20 km to the north of the northernmost mooring. (The map shown by S83 is different from the data set used to construct Figure 1, which shows only one such ridge.) S83 indicated there was some arbitrariness in these, statistically not always significant, results, as phase relationships were ambiguous over the 2π-cycle.

[6] In contrast with the findings by S83, most of later studies [cf. *Garrett*, 2001] suggested surface generation of near-inertial motions and subsequent downward propagation of near-inertial internal wave energy. *Maas* [2001] demonstrated theoretically that such downward propagating waves could focus energy near the bottom just above the critical latitude, where a complex pattern of upward and downward propagating waves was found. This could explain the results by S83. T. Gerkema and V. I. Shrira (Near-inertial waves in the ocean: Beyond the ''traditional approximation,'' submitted to *Journal of Fluid Mechanics*, 2004) (hereinafter referred to as Gerkema and Shrira, submitted manuscript, 2004) elaborated suggestions by *Saint-Guily* [1970] to demonstrate the possibility of near-bottom focusing of near-inertial energy at frequencies just below f ($\sigma \approx 0.99f$). Here these suggestions are verified using detailed spectral analysis. The present study is also part of the investigation questioning whether deep-ocean motions are mostly governed by random or quasi-deterministic internal wave signals, and part of the investigation on the spatial variation of internal wave coherency at a particular frequency, for example near and away from a source.

2. Data, Sites, and Methods

[7] Currents were evaluated from six moorings in an array near 33°N, 22°W (Table 1; Figure 1); see S83 for details. All moorings carried mechanical Aanderaa RCM-4 current meters that sampled once per hour. Three moorings consisted of three instruments at $\sim$10, 110, and 650 mab. The others had two instruments at $\sim$10 and 110 mab. Here we focus on the records from 110 mab to avoid problems related to the bottom boundary layer, estimated to extend between 20 and 120 mab (S83).

[8] Owing to the relatively low current speeds (typically $\leq$0.10 m s^{-1}) about 25–35% of the data were below the threshold level of $\sim$0.015 m s^{-1} due to stalling of the

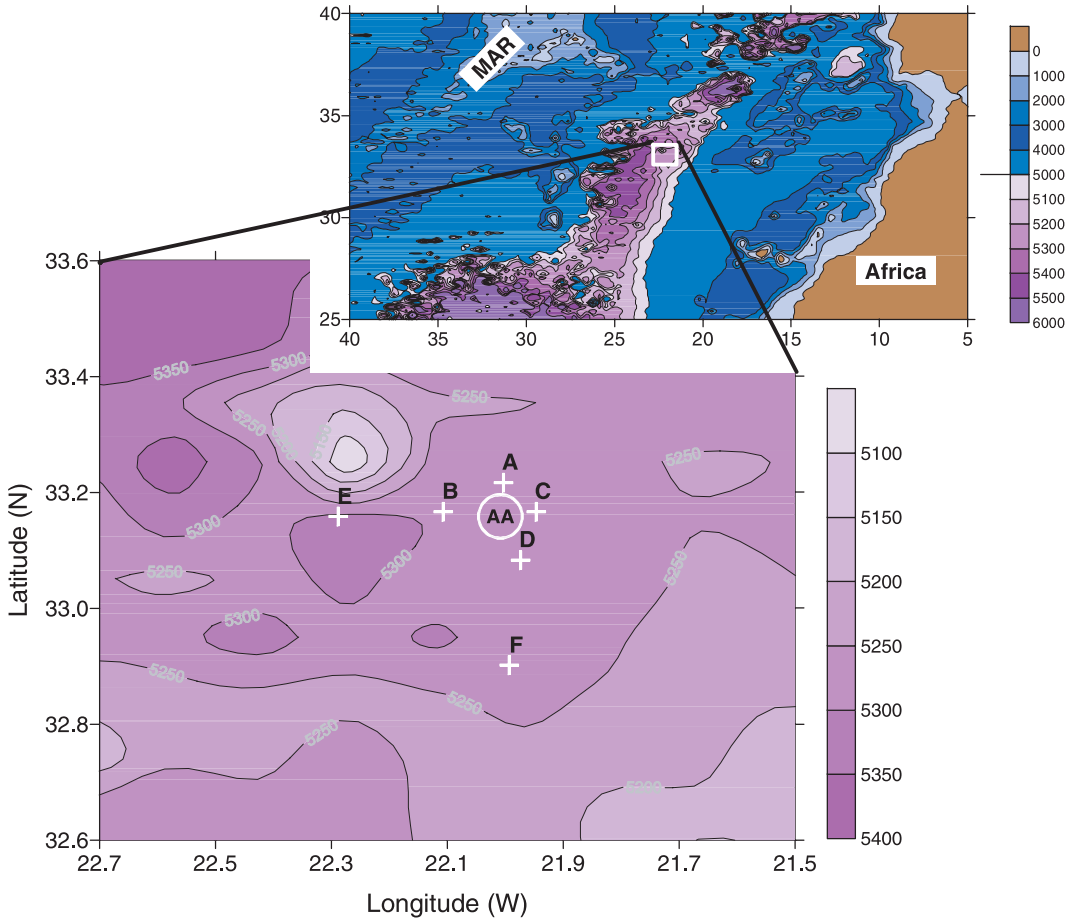

Figure 1. ETOPO2 (2′ grid interpolation) map of the Madeira abyssal plain to the north of the Canary Basin, with Madeira and Canary Islands to the right (roughly at −17°W) and the Mid-Atlantic Ridge (MAR) to the far left. Clearly, from the detailed contouring in 100-m contouring steps for depths between [5000, 5500] m, the abyssal "plain" shows numerous small ridges of several hundred meters in height. The detailed plot in 50-m contouring steps includes the different mooring locations (Table 1).

instruments. These instrumental flaws did not hinder the analyses, as remarked by S83. This was verified [*van Haren*, 2004a] using similar data from the abyssal Bay of Biscay after comparison with a test spectral model using artificial data and with records from more energetic regions higher up the continental slope in the Bay of Biscay. The artificial data consisted of a series of pure inertial and tidal harmonics that was truncated when speed fell below a certain threshold. This introduced some red noise and higher harmonics.

[9] The instruments' sampling was sufficient to resolve frequencies beyond local background N, which was estimated by S83 as N(4700) ≈ 5 cpd, N(5200) ≈ 3 cpd, slowly decreasing toward the bottom. Recent Seabird-911 CTD-profiles from locations in the Canary Basin ∼200 km to the south of the present moorings showed slightly lower values (Figure 2). This figure reflects relatively large variations of 20–30% in background N at each of the current meter depths: N(4700 ± 100 m) = 3.8 ± 0.8 cpd, N(5150 ± 100 m) = 1.8 ± 0.5 cpd using vertical length scale Δz = 25 m. Arguably, the latter value of N was close to the water column's minimum value (N_{min} ≈ 1.8 cpd). It is noted that variations were much larger when the vertical length-scale was reduced, so that the largest N found between 4600 and 5300 m was N_{max} ≈ 9 cpd using Δz = 5 m (Figure 2). This value was typical for the benthic deep ocean [*Armi and D'Asaro*, 1980].

[10] Spatial and temporal variations in background conditions like horizontal current shear and vertical stratification were expected to influence the internal wave spectrum. In the absence of horizontal shear in subinertial

Table 1. Moored Current Meter Data From the Abyssal Madeira Plain[a]

Mooring	Position N	Position W	Water Depth, m	Instrument Depth, m
A	33°13.0′	22°00.2′	5300	5287, 5186, 4642
B	33°10.0′	22°06.4′	5300	5288, 5187, 4643
C	33°10.0′	21°56.8′	5286	5273, 5173
D	33°05.0′	21°58.4′	5283	5271, 5172, 4630
E	33°09.5′	22°17.3′	5333	5321, 5220
F	32°54.1′	21°59.6′	5275	5263, 5163
AA	33°09.5′	22°00.5′		mean at 110 mab

[a]All instruments are Aanderaa RCM-4 sampled once per hour during 225 days between November 1980 and June 1981. Local inertial frequency f ≈ 1.09 cpd, and frequency is calculated in cycles per day (1 cpd = $2\pi/86400\ s^{-1}$). AA denotes the central position of the four moorings A, B, C, and D. Shortest horizontal distance A–C = 7.7 km, largest E–F = 39.6 km.

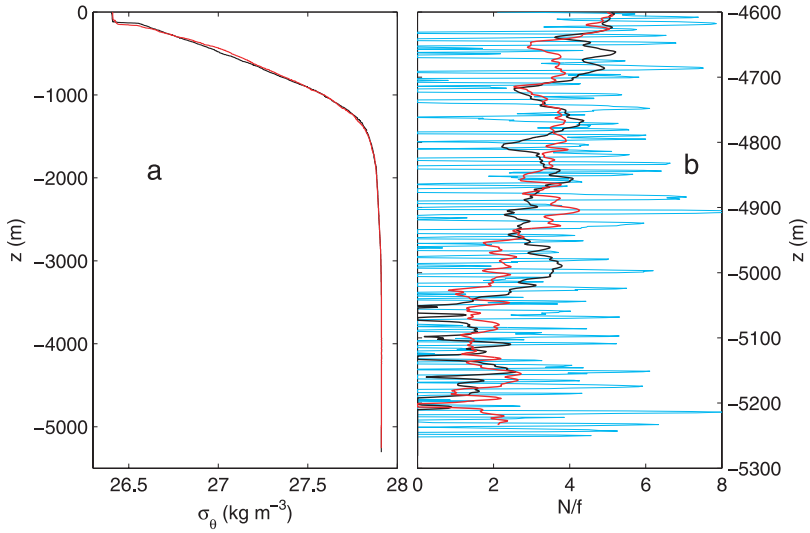

Figure 2. Two CTD profiles from the Canary Basin obtained at 30°00.0′N, 23°01.0′W using a Seabird-911 CTD in March 2003. (a) Density anomaly for the entire water column. (b) Near-bottom stratification relative to the local inertial frequency (f = 1.00 cpd). Original N ($\Delta z = 5$ m in blue) is smoothed over 50 m vertical intervals (red profile; in black is a second profile from data observed some time later).

motions, any variation in N results in: (1) a variation in internal gravity wave energy P(σ) as $P(\sigma) \sim N\sigma^{-p}$ following GM, (2) a variation of the free wave frequency range as N is the upper limit, (3) a change in the direction of propagation of internal gravity wave energy as the angle to the horizontal $\beta = \text{asin}[((\sigma^2 - f^2)/(N^2 - \sigma^2))^{0.5}]$, and (4) internal wave intermittency [*van Haren*, 2004b]; furthermore, in addition to the second result, for weak $N \rightarrow f$: (5) the inertio-gravity wave range $\alpha f < \sigma < N/\alpha$ ($0 < \alpha < 1$) extends well beyond the internal gravity wave frequency range $f < \sigma < N$ ($N \gg f$), [*LeBlond and Mysak*, 1978],

$$\begin{aligned}
&\alpha f < \sigma < N/\alpha,\\
&\alpha = \left(\sin^2\varphi\cos^2\nu - (\sin 2\varphi \sin 2\nu)/2\right.\\
&\quad \left. + \left(\cos^2\varphi + (N/2\Omega)^2\right)\sin^2\nu\right)^{0.5}/\sin\varphi\\
&\text{for } \nu = \text{atan}\left(\sin 2\varphi/\left(\cos 2\varphi + (N/2\Omega)^2\right)\right)/2. \qquad (3)
\end{aligned}$$

It follows from (3) that for N = 5.5 cpd α = 0.95, while for N = 1.8 cpd α = 0.70. As a result, the internal gravity wave band is extended due to the effects of inclusion of the horizontal component $2\Omega\cos\varphi$ of the Earth's rotational vector.

[11] In the spectral analysis performed here, variable smoothing was applied, 4–30 degrees of freedom (df). In order to examine spectral details, only a single cosine-bell shaped taper window was used only twice, half-overlapping, over the entire length of the time series without further smoothing (4 df). This weak smoothing resulted in an effective fundamental bandwidth $\delta\sigma_e \approx 4\delta\sigma_{fbw}$, with $\delta\sigma_{fbw}$ denoting the resolved fundamental bandwidth (~0.005 cpd for a 7-month record). Such nearly raw spectra are useful for some (e.g., tidal) motions that are deterministic rather than a particular realization of a stochastic process. Heavier smoothing was achieved by applying the same taper window over more than two half-overlapping subsections of the time series. Such smoothing was used to analyze nondeterministic signals, for example inertial motions and other nonharmonic internal wave band motions. Such signals are not random, as will be clear later, certainly not attributable to instrumental noise [*Briscoe*, 1975], and more likely due to varying background conditions [*van Haren*, 2004a]. However, conservatively, some statistics were invoked, as the spectral signature of varying background conditions and the measurements thereof is seldom precisely known.

[12] Two types of spectral analysis were computed. Kinetic energy spectra,

$$P_{KE}(\sigma) = P_-(\sigma) + P_+(\sigma), \qquad (4)$$

were the sum of the rotary current component spectra $P_-(\sigma)$, the clockwise spectrum, and $P_+(\sigma)$, the anticlockwise spectrum [*Gonella*, 1972]. In the (semi)diurnal tidal band these spectra also contained barotropic (surface wave) kinetic energy. The internal wave-character of motions within the frequency band (3) was demonstrated using the difference of the rotary spectra, for which Gonella introduced the "rotary coefficient,"

$$C_R(\sigma) = (P_-(\sigma) - P_+(\sigma))/P_{KE}(\sigma). \qquad (5)$$

C_R was equal to zero for purely rectilinear motion and equal to 1 for purely circular motion, its sign indicating the direction in which the horizontal current ellipse was traversed. Under symmetric forcing, the forcing being equal for both rotary components, and neglecting frictional stresses, the solution of (5) became,

$$C_R(\sigma) = \frac{2\sigma f}{\sigma^2 + f^2}. \qquad (6)$$

At frequencies within the internal wave band the solution (6) described free waves. For increasing frequencies as $\sigma \rightarrow N$ the near-rectilinear motions were viewed as circular

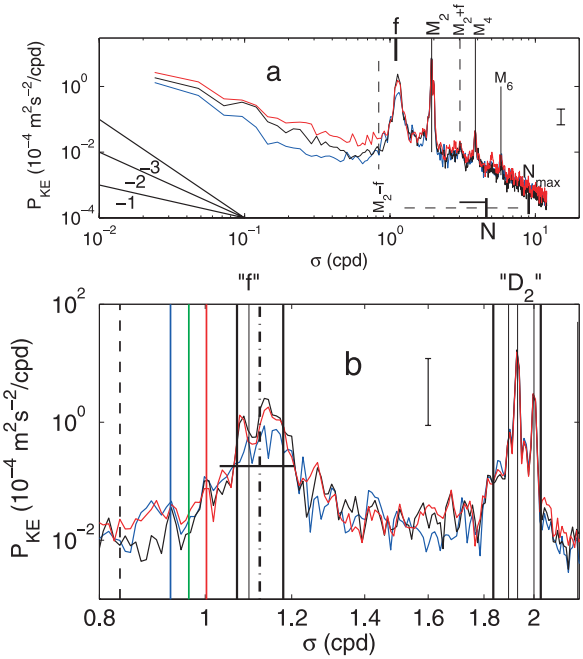

Figure 3. (a) Weakly smoothed (15 df, degrees of freedom; equivalent fundamental bandwidth $\Delta\sigma_{eq} \approx$ 0.05 cpd) kinetic energy spectrum from 225 days of current meter observations at 650 mab (m above the bottom; blue), 110 mab (black), and 10 mab (red) at mooring B in the Madeira abyssal plain (Figure 1; Table 1). Several spectral slopes with frequency (σ^p) are indicated by (p =) −1, −2, −3. Buoyancy frequency N is for 650 mab (average + 1 std; Figure 2) with the solid horizontal bar indicating 2 std and the dashed line the spread of original N (Δz = 5 m) data. (b) Detail of Figure 3a but for nearly raw (4 df, $\Delta\sigma_{eq} \approx$ 0.02 cpd) spectra. The vertical lines indicate frequencies from left to right: M_2-f (dashed line), O_1 (blue), M_1 (green), K_1 (red), 0.97f (thick solid line), f (thin solid line), 1.023f (dash-dotted line), 1.07f (thick solid line), 0.95M_2 (thick solid line), N_2 (thin solid line), M_2 (thin solid line), S_2 (thin solid line), 1.05M_2 (thick solid line). D_2 denotes the semidiurnal tidal band without specifying a single frequency. The horizontal solid line denotes the level of 0.1 times the peak value of the red spectrum in the band [0.9f, 1.1f]. In the error bar (95% statistical significance levels) the length of the horizontal lines indicates $2\Delta\sigma_{eq}$.

motions in a plane tilted progressively stronger from the horizontal.

3. Observations

3.1. Spectra at a Single Location

[13] In the lowest 650 m above the Madeira abyssal plain the kinetic energy spectra showed large energy in three frequency bands: subinertial ∼0.01–0.03 cpd, near-inertial, and semidiurnal tidal frequencies with the largest peak at the semidiurnal lunar frequency M_2 (Figure 3). In addition, within the internal wave band, peaks were observed at higher inertial-tidal and tidal-tidal harmonic frequencies, evidence of nonlinearity in the wave time series. Just inside the internal wave band (3), M_1 was indicated, which could have resulted from parametric subharmonic instability of M_2. However, this was not observed here. The spectral slope with frequency (σ^p) of the nonlinear internal wave band peaks was close to p = −3, which was observed previously [*van Haren et al.*, 2002]. These peaks were superposed on a nearly white (−1 < p < 0) continuum spectrum up to σ ∼ N. Because of the dominance of the tidal harmonics, a heavily smoothed spectrum had a slope p ∼ −2 for f < σ < ∼N. The kinetic energy spectra differed considerably toward the bottom, except for the peaks at M_2 (and to a somewhat lesser extent at S_2) that were identical to within ∼1% over the three current meters indicative of dominant large-scale, barotropic semidiurnal tidal motions as suggested previously (S83). Near f, more than twice as much near-inertial energy was found at 10 and 110 mab than at 650 mab. The maximum near-inertial energy was found at 110 mab, which was slightly larger energy than at 10 mab. Similar changes in variance by factors of 2–3 between 650 and 10/110 mab were observed between 0.03 < σ < 0.9 cpd, with most energy at 10 mab. At some internal wave frequencies, σ > S_2, largest energy was also found at 10 mab.

[14] Individual peaks were mostly not significant in a random statistical sense, except for the peaks at M_2 and, perhaps, at S_2. This statistical insignificance was somewhat surprising for the diurnal tidal constituents, although it could be argued that they were inside the inertio-gravity wave band (3) so that they were not exclusively barotropic motions, thereby adopting the viewpoint that internal waves are part of a random varying background. On the other hand, internal wave peaks that were consistent between the different instruments in the inertial band and at semidiurnal tidal sideband frequencies outside tidal constituent frequencies did not point at random variations. For these motions, common statistics were not readily applicable. This is elaborated in section 4.

[15] In the near-inertial band an apparent shift in frequency was observed with distance from the bottom (Figure 3b). At 650 mab the peak frequency $\sigma_p \sim 1.03$f, while at 10 and 110 mab this peak was more pronounced and a second peak was found at 0.99f, which was absent at 650 mab, where a tiny peak at 1.00f was found. Notwithstanding these peaks, the P_{KE}(f) had a fairly flat appearance, clearly defining a band with relatively sharp cutoffs so that the bandwidth $\Delta\sigma = (0.10 \pm 0.02)$f, at the levels where $P(\sigma_l) = P(\sigma_h) = 0.1P(\sigma)$, $\sigma_h - \sigma_l = \Delta\sigma$, and $\sigma_l < \sigma < \sigma_h$. This relative bandwidth was slightly larger, although well within the error bounds of the relative bandwidth found in observations from the Bay of Biscay [*van Haren*, 2004b].

[16] Except near the bottom, where N was occasionally very low albeit varying strongly with depth and, possibly, also with time (Figure 2), the internal wave band motions could be described using theory (6) for the band (3), although progressively less with decreasing N. This was inferred from the polarization spectra (Figure 4). Note the gap at semidiurnal tidal frequencies, evidence of rectilinear (barotropic) motions and confirming the findings by S83. Corresponding with the N decrease toward the bottom, largest internal wave band polarization was found at 650 mab for σ > 1.2f. In contrast with the gradual decrease with N with decreasing distance to the bottom, motions were most circular at the inertial frequency at 110 mab, where the largest near-inertial motions were found. Appar-

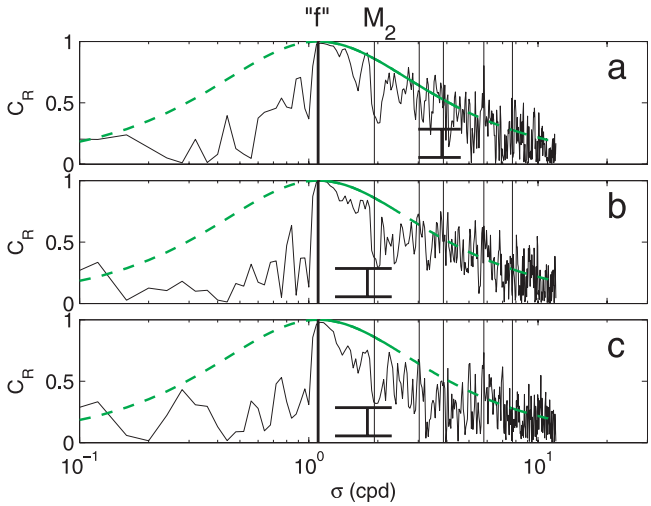

Figure 4. Moderately smoothed (30 df, $\Delta\sigma_{eq} \approx 0.09$ cpd) rotary coefficient $C_R(\sigma)$ as in (5) for records in Figure 3, with theory (6) in green, for (a) 650 mab, (b) 110 mab, and (c) 10 mab. The green line is solid within the internal gravity wave range $f < \sigma < N + 1$ std and dashed for other resolved frequencies. Vertical lines are at f, M_2, $M_2 + f$, M_4, M_6, and M_8. The horizontal lines of the error bar indicate $N \pm 1$ std.

ently, large-scale background stratification was non-zero over sufficiently large vertical scales, in contrast with observations from the western Mediterranean Sea where in the lower 600 m, N = 0 permanently and $C_R(f) = 0.3 \pm 0.2$ [*van Haren and Millot*, 2004].

[17] All the above observations were generally also made at the other moorings supporting three current meters at similar distances from the bottom, although subtle differences were noted.

3.2. Observations From Two Nearby Moorings

[18] The intensification of near-inertial energy toward the bottom noted by S83 was remarkable in some respects as it implied enhanced near-inertial energy with decreasing large-scale N (Figure 2). This was also observed in the Bay of Biscay [*van Haren et al.*, 2002]. Detailed nearly unsmoothed spectra of the near-inertial band from two nearby moorings with three current meters, A and D separated by 13 km, showed the same features as from mooring B: a distinct double near-inertial peak at 0.99/1.00f and at 1.02/1.03f at 10 and 110 mab, while a single peak at ~1.03f was found at 650 mab (not shown). It seemed that with an enhancement of near-inertial energy with decreasing large-scale N toward the bottom together with enhancement of subinertial energy, a red shift was observed to frequencies just below the local (planetary) inertial frequency. Such a shift to ~0.99f was also observed near the bottom in the western Mediterranean Sea, where the near-inertial peak was neither enhanced nor diminished with respect to mid-depth, well-stratified waters [*van Haren and Millot*, 2004].

[19] As to the cause of the above observation, suggesting trapping of near-inertial energy, we can only speculate. S83 suggested near-bottom generation, but alternatives can be proposed. The observed variation in subinertial energy could imply a change with depth of baroclinic subinertial vorticity ζ as could be inferred from streamline pattern observations by S83, yielding a change in effective local inertial frequency $f_{eff} = f + 0.5\zeta$ [*Mooers*, 1975] and thus the possibility of trapping of waves for $f_{eff} < \sigma < f$. The possibility for this to occur depends, naturally, strongly on the sign of ζ. Further alternative explanations of near-inertial energy trapping near the bottom are discussed in section 4.

3.3. O(10 km) Variations in the Horizontal Plane

[20] The blue (and possibly the red) shift in near-inertial frequency can be attributed to local vorticity modification of the frequency. Subinertial horizontal current differences of O(0.1 m s^{-1}/25 km) to yield $\zeta \sim \pm 0.02f$. Such values were readily observed (Figure 5). Similar variations were found at other frequencies. In section 3.4 it will be shown that such variations across O(30 km) also existed for tidal currents at the same energy level as variations in near-inertial currents, partially in contrast with the findings by S83. First, however, the effects were investigated of shorter-range horizontal variations on motions in various frequency bands.

[21] In the present analysis the mean records $(AA)_u$ and $(AA)_v$ were computed for each of the current components (u, v) from four moorings X = A, B, C and D (separated by ~10 km; Figure 1, Table 1) at a fixed height of 110 mab. $(AA)_u = (A_u + B_u + C_u + D_u)/4$, similar for v. The level of 10 mab was also analyzed for comparison, but results are not shown. Figure 6 demonstrates that the spectrum of AA (dropping subscripts) is more energetic than that of any of the residuals $X' = X - AA$, but for a few distinct frequency bands only: (1) $\sigma < 0.03$ cpd, (2) part of the near-inertial band, (3) the diurnal tidal constituents O_1 and K_1, and (4) the semidiurnal tidal constituents N_2, M_2, and S_2. Motions at all other frequencies, including those at inertial-tidal (e.g., $M_2 + f$) and tidal higher harmonics (e.g., S_4), were more energetic in the residual records. In statistical terms this implied short horizontal decorrelation scales <10 km at

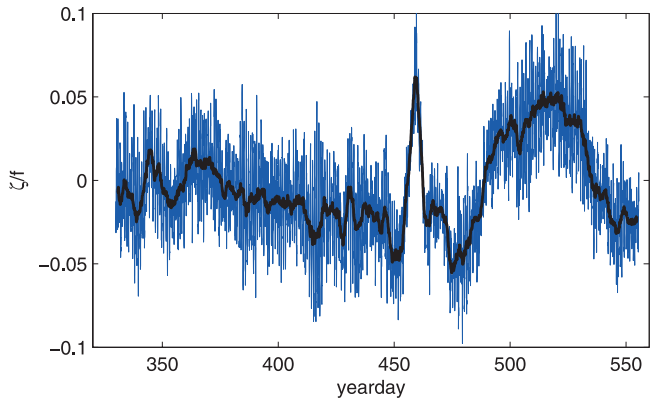

Figure 5. Time series of relative vorticity $\zeta = \Delta v/\Delta x - \Delta u/\Delta y$ at 110 mab normalized by local f and computed for the four closest moorings A, B, C, and D ($\Delta x \approx \Delta y \approx$ 15 km; Figure 1). In blue the original unfiltered time series is shown. In black is the daily averaged ("low-pass filtered") time series. Time is given in yeardays according to the convention that day 0.5 = 1200 UTC on 1 January, and days >365 are days in the following year.

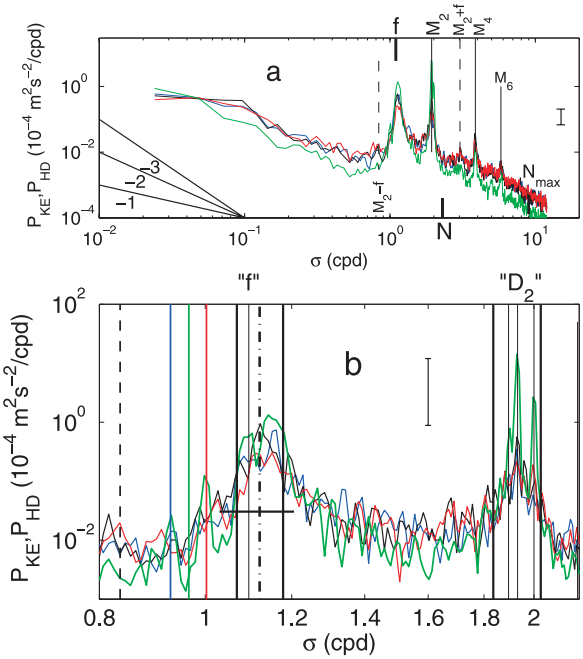

Figure 6. As in Figure 3 but for short-distance horizontal differences (P_{HD}) in current meter observations at 110 mab. Shown are the mean AA (green P_{KE} spectrum) of moorings A, B, C, and D (Figure 1; Table 1) and some residual signals: A′ = A-AA (blue P_{HD} spectrum), B′ (black P_{HD}), C′ (red P_{HD}).

most frequencies, confirming (2). In fact, the motions at these frequencies were dominated by large variations in phase between the different moorings.

[22] Some frequency dependence was observed in the discrepancy between residual and mean spectra: this discrepancy was large (∼a factor of 2, more or less according to expectations for random signals) for very high frequencies near the Nyquist frequency and less at inertial/tidal higher harmonics. The latter implied that phase variations were relatively large for higher harmonics compared to those of tidal and inertial motions, but they were smaller than for quasi-random signals as at their surrounding frequencies. It was noted that peaks at inertial-tidal harmonics extended to frequencies well beyond the large-scale estimate of N (maximum ∼3f locally) up to about short-scale N_{max}.

[23] In the mean for f and in all residuals for f, D_2 (denoting the semidiurnal tidal band without specifying a single frequency) and higher harmonics: $0.08 < \Delta\sigma/\sigma < 0.11$, delineating the borders of the band where the variance dropped to a tenth of the peak value. The $P_{KE}(M_2, S_2)_{AA} > P_{KE}(1.03f)_{AA}$, but $P_{KE}(M_2, S_2)_{X'} \leq P_{KE}(1.03f)_{X'}$ showing similar flat bands having similar relative bandwidths as observed in the Bay of Biscay [*van Haren*, 2004b].

[24] The different scales of motions dominating mean and residual spectra and the larger extent of the internal wave band beyond large-scale N, determined from CTD, could also be inferred from polarization spectra (Figure 7). The C_R for AA showed a gap around D_2 (Figure 7a), which did not exist in any of the residual signals (A′ was shown as an example in Figure 7b). At higher internal wave band frequencies $D_2 < \sigma < 4$ cpd AA and X′ differed in details only, until reaching spectral noise levels. This implied internal wave motions at horizontal scales $\Delta x < 10$ km and $\Delta x > 10$ km, according to (6). The most pronounced difference between AA and X′ was a banding of peaks-gaps of ∼0.9 cpd width in the X′-polarization spectra, less clear in $C_R(\sigma)_{AA}$, with peaks around f, M_2 + f, D_4, D_6, corresponding to the bands where the least discrepancy was found between AA and X′ in the kinetic energy spectra. It was noted that $C_R(f)_{AA} > C_R(f)_{X'}$ and that the subinertial flank dropped much steeper for AA than for X′. $C_{R,AA} = 0.5$ for $\sigma \approx 0.95f$, while $C_{R,A'} = 0.5$ for $\sigma \approx 0.82f$, approaching the value predicted using (3) for typical large-scale N. Hence, scale variations were frequency dependent, also within the near-inertial band.

[25] Near the bottom (10 mab) the C_R spectra showed the same features as above for f and D_2, but less polarization at all other IWB frequencies than observed for 110 mab.

3.4. O(30 km) Variations in the Horizontal Plane

[26] In order to investigate variations across several tens of kilometers, the mean AA, in which the part dominating short-scale (“incoherent”) variations was reduced due to the smoothing, was compared with records E (26 km due West of AA) and F (28 km due south of AA). At $\sigma < 0.03$ cpd the residual signals E′ and F′ were equal to or larger than the currents at AA (not shown). This implied large phase differences >90° across ∼30 km at these frequencies, confirming S83. At f, E′ and F′ were up to twice as energetic as AA (Figure 8a) so that similar or even larger phase differences applied as for $\sigma < 0.03$ cpd, as observed by S83. Furthermore, the peaked appearance in D_2 was a decade larger than X′(D_2) in the data presented in section 3.3 and only about half the energy at AA for M_2 and S_2 (except for E′) and ∼equal to AA’s energy for N_2 (Figure 8b). The much weaker diurnal motions are less peaked than in AA and comparable to those presented in section 3.3.

[27] Polarization in D_2 differed a lot between E′ and F′: approaching (6) for E′, while more rectilinear for F′ (Figure 9). Using harmonic analysis a scale of ∼100–300 km was estimated for the large-scale (barotropic?) major semidiurnal tidal constituent currents in the north(N)-south(S) direction, and ∼100–500 km in east(E)-west(W) direction. About half of the variations was due to changes in phase; the other half was due to changes in amplitude. They varied per constituent

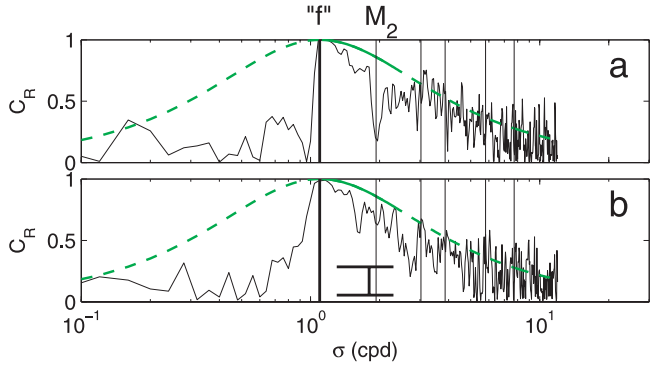

Figure 7. As in Figure 4 but for two records in Figure 6. (a) Average AA. (b) One example of the residuals (A′).

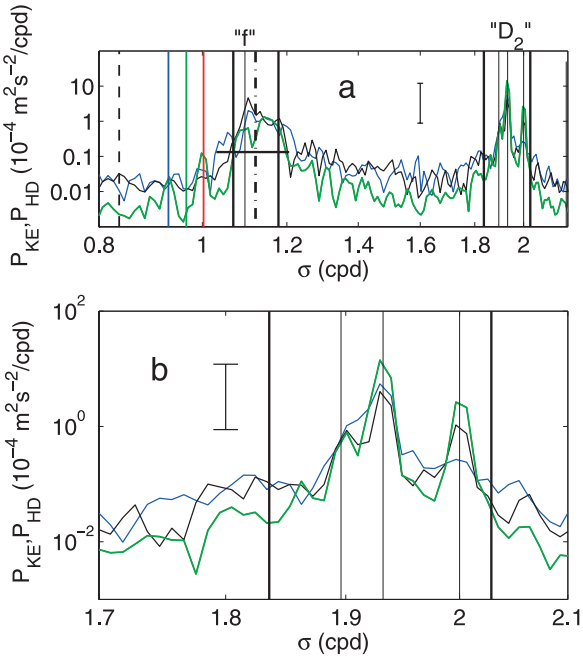

Figure 8. "Large"-distance horizontal (∼barotropic) differences (P_{HD}) in current meter observations at 110 mab. Shown are the (short-distance) mean AA (green P_{KE} spectrum) and residual signals: E′ = E-AA (blue P_{HD}) and F′ (black P_{HD}). (a) As in Figure 3b. The horizontal solid line denotes the 0.1 level times the peak value of the green spectrum in the near-inertial band. (b) Semidiurnal tidal band detail of Figure 8a. In the error bar in both panels the length of the horizontal lines indicates $2\Delta\sigma_{eq}$.

with generally smaller values for N_2 compared to M_2 and S_2. They were much larger than accepted for baroclinic, even mode-1, internal tidal motions. *Simmons et al.* [2004] estimated mode-1 baroclinic wavelengths of typically 100 km away from critical latitudes. Apparently, the "large-scale" tidal currents were influenced by local background conditions (topography, ζ and/or N).

[28] Resuming, although $P_{KE}(D_2) > P_{KE}(f)$ at a single location, the spectra of horizontal variations across ∼10 and 30 km showed that near-inertial motions became increasingly more important relative to tidal motions for decreasing horizontal distances. As we will see next, in the vertical this scale discrepancy between near-inertial and tidal motions is even more pronounced and near-inertial shear dominates the spectrum, not only in shelf seas [*van Haren et al.*, 1999] but also in the abyssal ocean.

3.5. Shear

[29] From the comparison between P_{KE} and the spectrum P_{vd} of the vertical difference record between data at 650 and 110 mab (∼Δz × **S**, shear **S** = (Δu/Δz, Δv/Δz)) it was seen that P_{KE} (110 mab) ≥ P_{vd} except in the bands $1.05 < \sigma < 1.45$ cpd, $\sigma > 7$ cpd ($\sim N_{max}$) and in the subinertial band $\sim 0.4 < \sigma < 0.95$ cpd (Figure 10). This implied a phase difference of more than 90° between the records at 110 and 650 mab for these exception frequency bands, and ∼180° ("maximum shear") when $P_{vd} = P_{KE,110} + P_{KE,650}$, for example near f. Phase differences of much less than 90° were inferred for $\sigma < 0.1$ cpd, D_2, and some D_4 frequencies.

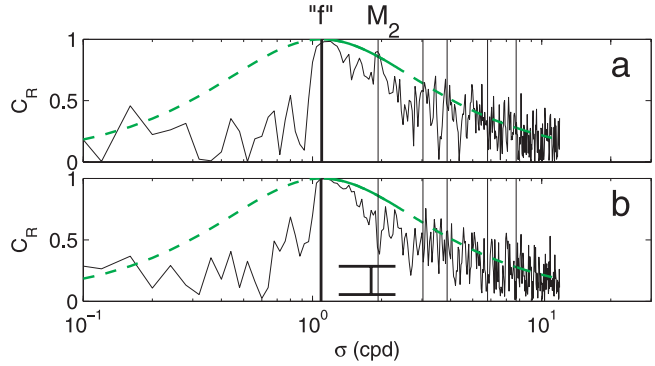

Figure 9. As in Figure 4 but for two records in Figure 8. (a) Residual E′. (b) Residual F′.

[30] In contrast with the spectra on horizontal variations, the P_{vd} spectrum was entirely dominated near f, again having a bandwidth very close to $\Delta\sigma = (0.10 \pm 0.02)$f and showing persistent peaks at ∼0.99f and 1.025f (Figure 10). The rest of the spectrum was rather flat and featureless compared to $P_{KE}(X)$ and $P_{KE}(X')$, except for a weak peak at D_2 and at some higher tidal harmonics. The spectral fall-off rate $P_{vd}(\sigma) \sim \sigma^p$ was $p \approx -0.5$ for $\sigma < 2f$ (excluding the band around f) and $p \approx -2$ for $\sigma > 2f \approx 2\Omega \approx N$. The dominance near f was reflected in the polarization spectrum (Figure 11): only in a band of ∼0.9 cpd width around f, between about [0.8, 1.7] cpd, and around M_2 + f and M_6 significant internal wave band polarization was observed, the rest suggesting "noise." Thus this **S**-spectrum reflected

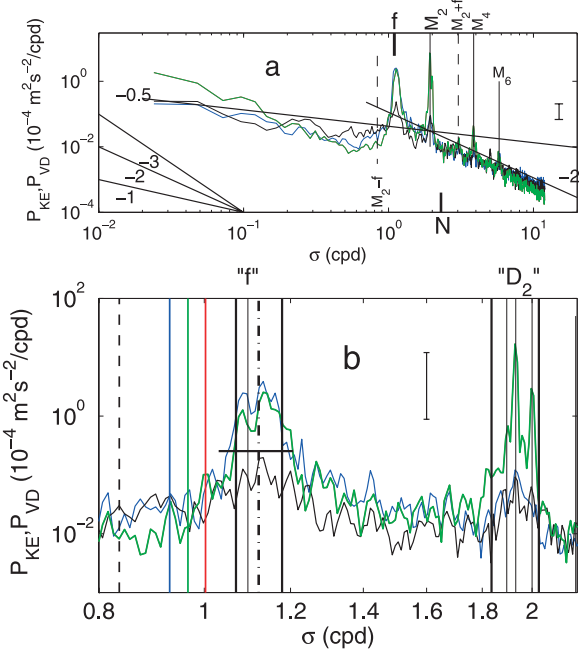

Figure 10. As in Figure 3 but for vertical differences (∼shear; P_{VD}) in current meter observations at mooring B referenced to the P_{KE} at B(110 mab) (green spectrum): 110–650 mab (blue P_{VD}) and 10–110 mab (black P_{VD}). In Figure 10b the horizontal solid line denotes the level of 0.1 times the peak value of the green spectrum in the near-inertial band.

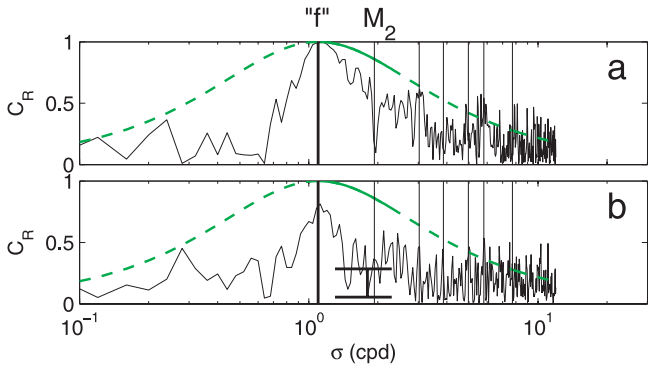

Figure 11. As in Figure 4 but for two records in Figure 10, for (a) 110–650 mab and (b) 10–110 mab. Vertical lines are at f, M_2, M_2 + f, M_4, M_4 + f, M_6, and M_8.

N (∼1.8 ± 0.4 cpd at 110 mab). Furthermore, the f-dominance implied circular shear (Figure 11a), so that its amplitude varied at much larger temporal scales (subinertial in frequency), like large-scale N.

[31] Between 10 and 110 mab, in the bottom boundary layer of varying height, the shear spectrum was similarly featureless (Figure 10). The lesser f peak was only marginally larger than the D_2 peak. When accounting for the vertical scale Δz (to transfer vertical current difference to shear) the bottom boundary layer S-spectrum was much larger than the one between 110 and 650 mab, except at f where values were comparable. Between 10 and 110 mab, polarization (Figure 11b) was even less than in Figure 4c.

4. Discussion

[32] The discussion in S83 on the apparent downward phase propagation of near-inertial motions demonstrates how complex the analysis can be of internal wave observations in varying background conditions. Although the suggested (S83) explanation of bottom generation of near-inertial internal waves is possible, presumably following relaxation of density fronts near the small bottom relief, upward energy propagation along near-inertial internal wave beams would certainly have "missed" the current meters at 10 mab. Also, it is somewhat difficult to comprehend that near-inertial internal waves generated at ∼5000 m depth showed largest energy in winter (Figure 5 of S83). In fact, this observation by S83 suggests time-dependent atmospheric forcing near the surface, although one would still need a transfer from near-surface wind generation to great depths. As a means to transfer energy to great depths, near-inertial motions could be generated via surface fronts [*Xing and Davies*, 2002; *Davies and Xing*, 2003], that is, via spatial differences in subinertial vorticity. It is noted that locally at great depths the observed subinertial background conditions such as ζ were sufficiently varying with time to explain the observed changes in near-inertial peaks.

[33] The observed split in peak frequencies 0.99f and 1.03f could be due to alternating blocking and trapping depending on the sign of ζ [*van Haren*, 2004a]. However, even with $\zeta = 0$, the red shift could imply a simple transfer from inertial energy in highly stratified waters near the surface to that in weakly stratified waters near the bottom. The red shift could be evidence of near-bottom focusing of near-inertial energy at $\sigma \sim 0.995$f due to the curvature of the Earth [*Maas*, 2001]. As the red shift was only weak, the observed peak still fell within the inertio-gravity wave range (3), and *van Haren and Millot* [2004] suggested dominant inertio (gyroscopic) wave propagation, and thus focusing. Gerkema and Shrira (submitted manuscript, 2004) modeled near-bottom trapping of energy at $\sigma = 0.99$f due to a smooth transfer from superinertial to subinertial frequencies when the horizontal component of the Earth's rotational vector was considered. As shown by *Saint-Guily* [1970] and Gerkema and Shrira (submitted manuscript, 2004), such subinertial motions have relatively small vertical length scales, making them a potential important factor for vertical shear and, thus, ocean mixing. Here we observed about the same shear at 0.99f and 1.03f, but we also noted a strong difference in polarization between motions at these near-inertial frequencies, while polarization of the shear was about the same. C_R was much more symmetric around f for shear than for currents.

[34] In contrast with highly deterministic tidal constituents, a single near-inertial peak did not exist in a statistically meaningful way, despite the aforementioned small "peaks." As a result, S83 could only use band-averaged phase and amplitude relationships on near-inertial energy propagation. On the other hand, although the near-inertial band lacked a deterministic peak, it had a finite width in frequency, which determined the intermittent appearance of near-inertial motions in the time domain [*van Haren*, 2004b]. This intermittency seemed random, as for example evident in the definition of "incoherent" internal (tidal) motions [*van Haren*, 2004a]. However, one can argue that a purely statistically incoherent signal, also defined as a random signal, cannot describe finite-bandwidth near-inertial and tidal internal wave signals: statistics cannot explain "intermittency," a property typical for internal waves occurring in groups. A better definition of the latter would be a "peak-intermittent signal" or a "quasi-deterministic incoherent" signal. With the help of the observations presented in this paper, we may continue the discussion on the quasi-statistics of internal wave motions, which was started for internal tidal motions by *van Haren* [2004a].

[35] In the Madeira abyssal plain, deep-ocean motions seem to be organized around three particular groups of frequencies: very low frequency (subinertial), near-inertial, and semidiurnal tidal. Motions within these groups have their specific spatial scales, which are larger than at other frequencies but which are much less than the ocean-basin scale, even for the tides, and more like the smallest topographic scales. It is hypothesized that these spatial scales lead to the possibility for small-scale current variability and thus relatively strong nonlinear interactions that subsequently govern motions at frequencies outside the three bands mentioned above, thereby filling the entire spectrum. This filling is not equal for all frequencies and will lead to specific enhanced bands, such as higher tidal harmonics and tidal-inertial interaction frequencies. Such banding of ∼0.9 cpd width within the internal wave band was noticed in polarization spectra from the Bay of Biscay by *van Haren* [2003]. It was also visible in coherence spectra of vertical velocity in IWEX data (bands of ∼0.04 cph = ∼1 cpd with peaks at inertial-tidal harmonics

in, for example, Figures 9 and 11 of *Briscoe* [1975]) when instrumentation separation is larger than several 100 m horizontally. The motions in these bands had larger scales than at surrounding less energetic frequencies. These scales were comparable to those of internal inertial and tidal motions.

[36] This effect of different spatial scales suggests that a motion registered at a fixed position in space cannot be comparable to the one registered some distance away. Phase differences are larger than a few degrees as soon as particles move outside an imaginary box with horizontal scales of ~1000 m and ~10 m vertically. The latter vertical scale is peculiar as it sets the stratification scale for internal wave band coherence, as noted by *Siedler* [1971]. It is also the canonical scale for deep-ocean shear that is dominated at f, so that near-inertial motions are important for the entire internal wave band.

[37] Thus, as discussed in Appendix A, the spectra from two current meter records at different moorings may look identical; detailed inspection of spectral variations demonstrates that the differences between the records, previously called statistical error, are at the same level as the individual spectra. All ''incoherency'' is not instrumental but mainly due to effects in background conditions. These cause phase and amplitude differences: Vertical current shear is governed by near-inertial motions, while horizontal variations are governed by subinertial, near-inertial, and semidiurnal tidal motions, although each at different scales. Such horizontal variations affect the strength of nonlinear advection and thus of the dominating internal wave band signals. A spectrum of a long Eulerian record is a consequence of several short-term deterministic signals propagating in nonlinear groups through a varying background.

[38] As outlined in Appendix A, the above has consequences for the construction of long time series from the matching of consecutive records at nearby moorings. Unfortunately, logistical problems do not allow for deployments of moorings that cover about the entire water column within the required horizontal distance of only ~0.1H.

5. Summary and Conclusions

[39] Spectral analysis of a set of deep-ocean current data from relatively closely spaced moorings showed that the dominant motions, at subinertial, near-inertial, and semidiurnal tidal frequencies, varied on relatively short spatial scales O(10–300 km) horizontally and several hundred meters vertically. These scales were larger than at frequencies outside these bands and barely smaller than typical scales for shallow seas. The larger scales were typical for ''barotropic'' or ''large-scale'' tidal motions. They seemed related to topographic variations of ridges of several hundred meters in height on the abyssal plain, which was considered flat hitherto. The 300-km scale was much larger than estimated for mode-1 internal tidal waves. This suggested dominance of barotropic motions, which was confirmed by the analysis of polarization of horizontal currents. The shorter length scales were for the subinertial, near-inertial, and ''small-scale'' tidal motions. The latter dominated horizontal advection scales, while at some distance above the bottom, near-inertial motions completely dominated vertical shear. As near-inertial motions were very nearly circularly polarized, the shear magnitude varied only slowly with time, as found previously in shallow seas. Here strong near-inertial shear was found at superinertial frequencies 1.03f and at subinertial frequencies 0.99f due to trapping of motions at these frequencies in weakly stratified waters near the bottom.

[40] Future studies on varying background effects on internal wave motions require very long time series, well exceeding 1 year of observations, to distinguish between the various quasi-deterministic and quasi-statistic motions. They are also useful to infer climatic variations in the background conditions, from inspection of the energy in the different parts within the internal wave band. Such very long time series should be purely Eulerian and therefore from a single mooring position using instruments equipped with extended batteries and memory capacity to avoid spectral smearing of results.

Appendix A: Composite Time Series of Observations From Nearby Moorings

[41] We are interested in constructing long time series beyond the limitation of instrumental power supply and data storage capacity. A common method is to deploy an identical mooring as close as possible to a previous one, preferably a few days prior to recovery of the latter to achieve overlap of time series. In practice, using common single line moorings without special handling (e.g., ROV) equipment moorings cannot be located nearer to each other than 1–2 times the mooring length and/or the local water depth, to avoid entanglement. As a result, some of the moorings considered here are among the closest ever deployed together in water of depth ~5 km. However, as indicated in section 1 and as demonstrated in section 3, instruments on deep-ocean moorings separated by horizontal distances of ~10 km show different spectral results commensurate with the natural variability in motions at nearly all frequencies. The dramatic effects on the construction of long time series may be appreciated by the following exercise.

[42] At a single depth level (110 mab), records from the two nearest moorings (A and C) in the present study were split in half,

$$u_{A,110}(t = 1, \ldots, T) = u_{A1,110}(t = 1, \ldots, T/2) + u_{A2,110}(t = T/2 + 1, \ldots, T), \quad (A1)$$

with T denoting the total sampling period of units t, and similar for v and for currents at mooring C. Then the halved records were matched with halves from the other mooring, as if the first half was measured by an instrument at the first mooring and the second half by an instrument at a mooring deployed near the first, for instance,

$$u_{test1} = u_{A1} + u_{C2} \quad (A2)$$

$$u_{test2} = u_{C1} + u_{A2}, \quad (A3)$$

and similar for v. The above was also performed for data from 10 mab for reference. As results were similar, we only discuss depth level 110 mab below.

[43] Figure A1 shows an example of the resulting time series (A2), with a large change in current between the two halves. It is noted that these moorings were at the Madeira abyssal plain, a deep-ocean site known for its relative lack of large topographic variations and weak variations in density and horizontal shear. It may be clear that it would have been virtually impossible to adequately match time series from different instruments at two such nearby moorings, even when a proper overlap in time series was allowed. This was caused by the current variation across short horizontal spatial scales.

[44] In the amplitude variance spectra (Figure A2) this was visible in the variations at the level of observations in nearly every frequency band, except at some harmonic tidal frequencies. Commonly, such variations were attributed to unspecified "spectral noise," and demonstrating "errors" were large, as followed after comparison with statistical (χ^2-distribution) models. However, this unspecified noise, not being random, reflected phase changes in currents induced by the effects of the varying background conditions of subinertial vorticity and stratification and their interaction with internal waves [*van Haren*, 2004b]. Here, most importantly, it is shown that it is difficult to construct long current meter time series beyond limitations of power supply and memory capacity.

[45] One could elaborate on the above and question what the effects might be (1) higher in the water column and (2) of a "swaying mooring," although the associated horizontal displacements O(100–1000 m) are seldom more than 20% of the mooring line length. Such distances are an order of magnitude smaller than the distance between the moorings considered here, but they were typical for upper water column IWEX [*Briscoe*, 1975] and site D (~920 m) [*Siedler*, 1974]. As for case 1, the results presented by *Briscoe* [1975] and *Siedler* [1974] show a drop in horizontal coherence below the statistical significance level at $\sigma \approx$ 10 cpd (for separation distance 920 m) and $\sigma \approx 4$ cpd (for separation distance 1600 m). This is similar to the near-bottom findings presented in this paper. Together with the IWEX result that coherence drops below the statistical significance level at $\sigma \approx 100$ cpd for separation distance 44 m and at $\sigma \approx 40$ cpd (~local N) for 450 m, it is probably safe to say that mooring motions do not affect the internal wave band spectrum for typical N provided they are limited within angles <10° in the vertical.

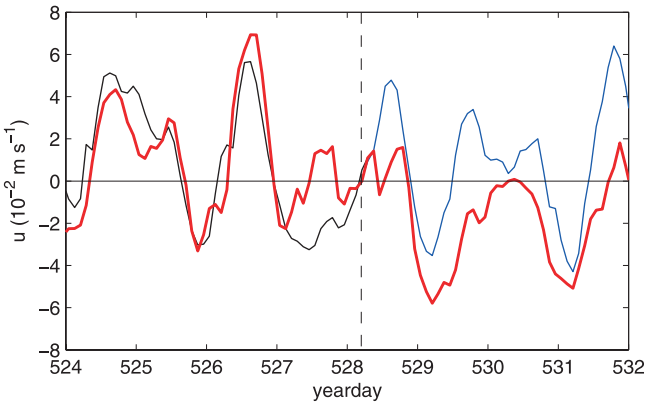

Figure A1. Detail near the middle (vertical dashed line) of time series of u-current component observed at 110 mab of the two closest moorings A (blue) and C (black) (distance 7.7 km = 1.5H). In red is the artificial record constructed from the first half of A and the second half of C. The v-component shows similar results.

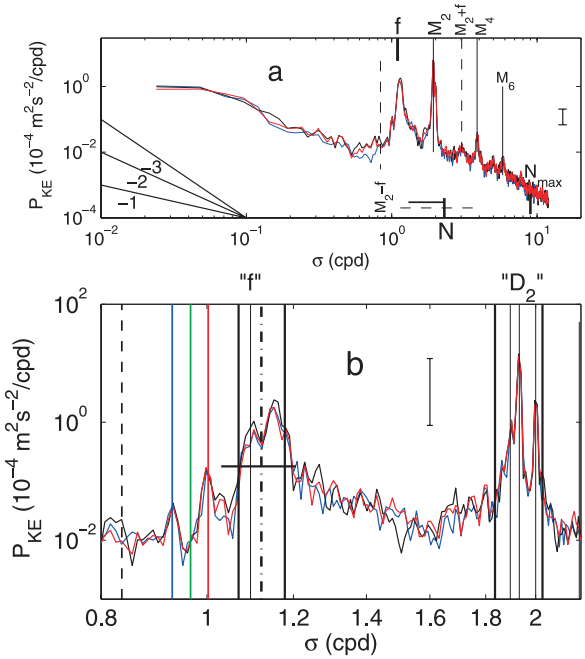

Figure A2. As in Figure 3 but for the records of which the u-component was shown in Figure A1: artificial record (red spectrum), A (blue), and C (black). In Figure A2b the horizontal solid line denotes the level of 0.1 times the peak value of the red spectrum in the near-inertial band.

[46] **Acknowledgments.** I thank the crew of the R/V *Pelagia* during the LOCO-IW cruise during which the CTD-data of Figure 2 were obtained. Margriet Hiehle composed Figure 1. The moored current meter data were obtained by IOS Wormley, UK, and are made easily accessible by OSU's buoy group, Corvallis, Oregon, USA.

References

Armi, L., and E. D'Asaro (1980), Flow structures of the benthic ocean, *J. Geophys. Res.*, *85*, 469–483.

Briscoe, M. G. (1975), Preliminary results from the trimoored internal wave experiment (IWEX), *J. Geophys. Res.*, *80*, 3872–3884.

Davies, A. M., and J. Xing (2003), On the interaction between internal tides and wind-induced near-inertial currents at the shelf edge, *J. Geophys. Res.*, *108*(C3), 3099, doi:10.1029/2002JC001375.

Garrett, C. (2001), What is the "Near-Inertial" band and why is it different from the rest of the internal wave spectrum?, *J. Phys. Oceanogr.*, *31*, 962–971.

Garrett, C. J. R., and W. H. Munk (1972), Space-time scales of internal waves, *Geophys. Fluid Dyn.*, *3*, 225–264.

Gonella, J. (1972), A rotary-component method for analysing meteorological and oceanographic vector time series, *Deep Sea Res.*, *19*, 833–846.

LeBlond, P. H., and L. A. Mysak (1978), *Waves in the Ocean*, 602 pp., Elsevier Sci., New York.

Maas, L. R. M. (2001), Wave focusing and ensuing mean flow due to symmetry breaking in rotating fluids, *J. Fluid Mech.*, *437*, 13–28.

Mooers, C. N. K. (1975), Several effects of a baroclinic current on the cross-stream propagation of inertial-internal waves, *Geophys. Fluid Dyn.*, *6*, 245–275.

Munk, W., and C. Wunsch (1998), Abyssal recipes II: Energetics of tidal and wind mixing, *Deep Sea Res., Part I*, *45*, 1977–2010.

Saint-Guily, B. (1970), On internal waves: Effects of the horizontal component of the Earth's rotation and of a uniform current, *Dtsch. Hydrol. Z.*, *23*, 16–23.

Saunders, P. M. (1983), Benthic observations on the Madeira abyssal plain: Currents and dispersion, *J. Phys. Oceanogr.*, *13*, 1416–1429.
Siedler, G. (1971), Vertical coherence of short-periodic current variations, *Deep Sea Res.*, *18*, 179–191.
Siedler, G. (1974), Observations of internal wave coherence in the deep ocean, *Deep Sea Res.*, *21*, 597–610.
Simmons, H. L., R. W. Hallberg, and B. K. Arbic (2004), Internal wave generation in a global baroclinic tide model, *Deep Sea Res., Part II*, *51*, 3043–3068.
van Haren, H. (2003), On the polarization of oscillatory currents in the Bay of Biscay, *J. Geophys. Res.*, *108*(C9), 3290, doi:10.1029/2002JC001736.
van Haren, H. (2004a), Incoherent internal tidal currents in the deep ocean, *Ocean Dyn.*, *54*, 66–76.
van Haren, H. (2004b), Bandwidth similarity at inertial and tidal frequencies in kinetic energy spectra from the Bay of Biscay, *Deep Sea Res., Part I*, *51*, 637–652.
van Haren, H., and C. Millot (2004), Rectilinear and circular inertial motions in the western Mediterranean Sea, *Deep Sea Res., Part I*, *51*, 1441–1455.
van Haren, H., L. Maas, J. T. F. Zimmerman, H. Ridderinkhof, and H. Malschaert (1999), Strong inertial currents and marginal internal wave stability in the central North Sea, *Geophys. Res. Lett.*, *26*, 2993–2996.
van Haren, H., L. Maas, and H. van Aken (2002), Construction of "internal wave" spectrum near a continental slope, *Geophys. Res. Lett.*, *29*(12), 1615, doi:10.1029/2001GL014341.
Xing, J., and A. M. Davies (2002), Processes influencing the non-linear interaction between inertial oscillations, near inertial internal waves and internal tides, *Geophys. Res. Lett.*, *29*(5), 1067, doi:10.1029/2001GL014199.
Webster, F. (1972), Estimates of the coherence of ocean currents over vertical distances, *Deep Sea Res.*, *19*, 35–44.

H. van Haren, Royal Netherlands Institute for Sea Research (NIOZ), P.O. Box 59, NL-1790 AB Den Burg, Netherlands. (hansvh@nioz.nl)